Front. Earth Sci. 2022, 16(1): 5–16
https://doi.org/10.1007/s11707-020-0866-5

RESEARCH ARTICLE

Quantifying interagency differences in intensity estimations of Super Typhoon Lekima (2019)

Lina BAI (✉)[1], Jie TANG[1], Rong GUO[1], Shuai ZHANG[1], Kaiye LIU[2]

1 Shanghai Typhoon Institute of China Meteorological Administration, Shanghai 200030, China
2 Shanwei Meteorological Observatory, Shanwei 516600, China

Abstract There were significant discrepancies in the intensity estimations of Super Typhoon Lekima (2019) among the China Meteorological Administration (CMA), the United States Joint Typhoon Warning Center (JTWC), and the Japan Meteorological Agency (JMA) data sets, with a maximum difference of over 12 m/s and 16 m/s between the JTWC data set and the CMA and JMA data sets, respectively. During the intensification phase, disagreement on the maximum sustained wind (MSW) between these agencies was due to the use of different conversion tables for the current intensity number (CI) estimated by Dvorak technique-MSW. In addition, CI discrepancies and different available observational data were also important contributors to the different intensities estimated during the Lekima's decay phase before landfall. The ability of various methods to minimize these discrepancies was evaluated in this study. Both the linear factor multiplication method and the remapping method using the same CI-MSW conversion table have substantially abilities to reduce intensity discrepancies, with the latter method being more effective. However, these improvements only hold for the intensification phase in the ocean. The CMA data set had more complete and accurate intensity estimations when Lekima made landfall in China. After its landfall, the intensity estimate of the CMA was comparable to that of the JMA, which differed greatly from that of the JTWC.

1 Introduction

Given the serious damage to people and the economy caused by tropical cyclones (TCs), many operational centers provide TC best track database. For TCs occurring in the North-west Pacific, best track data sets including information on TC intensity and location are provided by four forecast centers, namely the Shanghai Typhoon Institute of China Meteorological Administration (CMA/STI), the Hong Kong Observatory (HKO), the United States Joint Typhoon Warning Center (JTWC), and the Japan Meteorological Agency (JMA). Tropical cyclone (TC) intensities recorded in the best track data are defined as the maximum sustained wind (MSW) at 10-m height and the minimum sea-level pressure (MSLP).

Previous studies found significant discrepancies between the historical best track data sets of these agencies and have investigated the differences in their TC intensity trends (Wu et al., 2006; Song et al., 2010; Ying et al., 2011; Kang and Elsner, 2012). Song et al. (2010) found an increasing trend in the annual frequency of strong TCs during 1977–2007 in the JTWC data set, but decreasing trends in the CMA and JMA data sets; this was later confirmed by Ren et al. (2011). Yeung (2006) and Wu et al. (2006) also found that there was no increase in the activity of intense TCs in the JMA and HKO data sets, in contrast to the JTWC data set. Other literature has focused on mean interagency discrepancies in different decades (Yu et al., 2007; Knapp and Kruk, 2010; Ren et al., 2011; Barcikowska et al., 2012). Ren et al. (2011) noted that TC intensity discrepancies were smallest between the CMA, JTWC, and JMA data sets during 1973–1987, whereas large discrepancies occurred during other periods. The TC intensity was overestimated during the period prior to the early 1970s in the CMA best track data set, but was overestimated in the JTWC data set after the termination of aircraft observations. Yu et al. (2007) compared the data sets of the CMA, JTWC, and JMA and found that there were remarkable intensity discrepancies, with a maximum difference for the same TC of more than 30 m/s.

Given the obvious intensity discrepancies between these data sets, the reasons for these differences need to be discussed and documented. Previous studies have found that the differences in the MSW estimation between these

Received July 15, 2020; accepted December 20, 2020

E-mail: bailn@typhoon.org.cn

agencies are the result of at least two factors (Knapp and Kruk, 2010; Song et al., 2010). One factor is that the MSWs are averaged over different time intervals. The MSWs in the JTWC data set are averaged over a 1-min period, while MSWs in the JMA and CMA best track data sets are calculated by averaging the wind speed over a 10-min and 2-min period, respectively. The other factor is that different principles and input observational data are used by these operational centers to determine the MSW.

Previous studies comparing TC intensity data sets have mostly focused on long-term trends and average discrepancies over different decades. However, the observational techniques and analysis procedures for intensity estimations have varied during the last several decades. For example, the wind-pressure relationship (WPR) suggested by Knaff and Zehr (2007) has replaced that of Atkinson and Holliday (1977) for operational TC intensity estimations at the JTWC since 2007 (U. S. Fleet Weather Facility, 2007; Bai et al., 2019). The CMA improved the operational flow of TC intensity estimations and adopted the technique of Dvorak (1984) recommended by the World Meteorological Organization since 2013 (Xu et al., 2015). Therefore, it is necessary to compare interagency differences in intensity estimations of the TCs that have occurred in recent years and to analyze the reasons for those differences.

This study concentrates on Typhoon Lekima (2019), which made landfall in China three times. The first and most devastating landfall was in the Zhejiang Province at 17:45 UTC on 9 August 2019, with observed peak instantaneous wind speeds of 61.4 m/s and a 2-min averaged maximum wind speed of 50.5 m/s near the landfall location. It brought strong winds and heavy rainfall to coastal provinces from the Fujian Province up to the Heilongjiang Province (Yu and Chen, 2019). This paper answers the following questions to better understand the interagency discrepancies in intensity estimations of Lekima:

1) What are the interagency differences in MSW during the different phases of Lekima?

2) Do differences in the analysis and operating procedures between agencies account for these MSW differences? Are there some methods that can decrease interagency discrepancies in TC intensity estimations?

We note that previous studies discussing the intensity discrepancies in different best track data sets did not separate the samples into those occurring over water and over land. However, different procedures are performed depending on whether TCs are located over land or oceans, because of the different available observational data. The MSW is usually estimated based on satellite images over the open ocean area, since buoys and other in situ observations are unavailable. However, TC intensity over land is estimated based on surface station observations. For offshore TCs, the intensity is usually analyzed using several sources of data, including in situ observations, radar data, and satellite images. In this study, we therefore split the best track data according to when Lekima was over the ocean and over the land to better understand how interagency differences in its estimated intensity can be reduced.

2 Data and methods

The TC best track data sets used here are provided by the CMA/STI (available at CMA Tropical Cyclone Data Center website), the JMA (available at Japan Meteorological Agency), and the JTWC (available at The Tropical Cyclone Best Track Data Site of JTWC website). The JTWC data set contains the TC center, MSW, and MSLP at 6-h intervals during the whole lifespan of Lekima. The JMA data set includes 6-hourly track and intensity analyses of MSW and MSLP, except from 18:00 UTC on 7 August to 00:00 UTC on 9 August, when the data are at 3-h intervals. The CMA track and intensity records of MSW and MSLP are 3-hourly from 24 h before Lekima's landfall in China to the time it moves away from China; otherwise, the time interval is 6-hourly. The MSW values in the CMA and JTWC data sets are recorded when the intensity reaches that of a tropical depression (TD), whereas the JMA does not include MSW values for TDs. In addition, the CMA also provides specialized information for TCs that make landfall in China, including the TC number, landfall time, landfall location, and the intensity at landfall in terms of MSW and MSLP. For example, Lekima (TY Number 1909), made landfall in China three times: first in the Zhejiang Province, with a MSW of 52 m/s, a number 16 on the Beaufort scale, and a MSLP of 930 hPa, and then twice in the Shandong Province, with MSWs of 23 m/s, and a MSLP of 980 hPa and 984 hPa, respectively (Table 1).

Table 1 Landfall information for Lekima (2019) in the CMA TC database

TY number	Landfall events		Location of landfall (County, Province)	Data and time (mmddhhnn/UTC)	Intensity at landfall		
	Total	No.			BS	m/s	hPa
1909	3	1	Wenling, Zhejiang	08091745	16	52	930
	3	2	Qingdao, Shandong	08111250	9	23	980
	3	3	Changyi, Shandong	08120300	9	23	984

Note: BS = Beaufort scale.

Over the open ocean, TC location and intensity estimations primarily depend on satellite data analysis, including infrared/visible cloud image and microwave data (Dvorak, 1975, 1984; Olander et al., 2004; Olander and Velden, 2007; Lu and Yu, 2013; Lu et al., 2019). Among the various techniques, the Dvorak technique (Dvorak, 1975, 1984; Velden et al., 2006) has been the primary method used to estimate TC intensity for more than 40 decades. The procedure is as follows. First, a T-number is derived based on the cloud patterns in satellite images. Then a current intensity (CI) number is determined from the T-number using procedural rules which reduce the daily variation in TC intensity. Lastly, the MSLP and MSW are estimated by using a conversion table between CI number and TC intensity. However, the analysis procedures used to estimate the CI from satellite data are different in some details between different operational centers. In addition, the CI–MSW conversions were also established independently at each operational agency. The JTWC adopted the CI–MSW conversion table originally used by Dvorak (1984). The JMA designed a new conversion table (Koba et al. 1991) that transfers CI parameters directly to the 10-min MSW and MSLP. Before 2013, the CMA established a method similar to the original Dvorak approach (Group of Satellite Imagery Analysis, 1980a, b) to estimate TC intensity, which used a CI–MSW conversion table calculated from real-time satellite image analyses (Ying et al., 2014). The standard Dvorak technique (Dvorak, 1984) has been adopted by the CMA since 2013 (Xu et al., 2015). The CI–MSW conversions were changed based on the reanalysis of the relationship between CI number and MSW values of the historical CMA TC best track data set. The CI–MSW conversions used by the JTWC, JMA, and CMA are shown in Fig. 1. In addition, the MSLP in the CMA and JTWC data sets are obtained according to a WPR. The JTWC has adopted the WPR suggested by Knaff and Zehr (2007) since 2007. The CMA have changed the WPR twice, once in 1972 and again in 2013 (Ying et al., 2014; Xu et al., 2015). The MSLP in the JMA data set is obtained via a CI–MSLP conversion table (Koba et al. 1991).

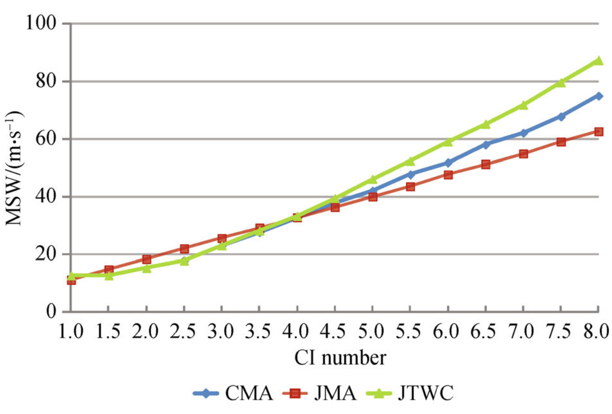

Fig. 1 Conversions for the Dvorak-derived CI number and MSW used by the CMA, JTWC and JMA. The blue line for CI numbers less than 4 is hidden behind the green line.

Both the MSW and MSLP in the CMA data set are determined using surface station observations when TCs are over land in China. For offshore TCs, the intensity is usually estimated by taking all the collected data into consideration, including surface observations, radar data, satellite images, and buoy data. In 2012, the number of national reference climatological surface stations and automatic weather stations in China increased to 2411 and 31819, respectively (Liu, 2015). The Doppler radar network covers the entire land area and coastal waters of China impacted by TCs (Ying et al., 2014). However, the number of surface weather stations participating in international exchange activities is less than 50 in the coastal provinces and cities of China (CMA, 2012). The JTWC and JMA estimate the intensity of TCs near the coast of China primarily based on satellite analysis.

To evaluate the intensity estimations of these three data sets, we used additional objective TC intensity estimation techniques as a reference. The advanced Dvorak technique (ADT), developed by the Cooperative Institute for Meteorological Satellite Studies (CIMSS) (available at CIMSS website), is a widely used objective algorithm for calculating TC intensity. The ADT strives to reduce the subjective analysis procedure and extend the method beyond the original Dvorak technique (Olander and Velden, 2007). The digital Dvorak intensity estimates (DDIE) developed by Zehr (1989) is another objective technique using enhanced infrared satellite data. It was found that the DDIE method performs effectively when TCs are well-organized when TCs are strong and well-organized. (available at Regional and Mesoscale Meteorology Branch website). We also used ASCAT surface wind data (available at NOAA website) to evaluate which data sets provide more accurate MSW estimations. We used the ASCAT ocean surface winds with a spatial resolution of 25 km (Sivareddy et al., 2013). The wind speed range is 0–50 m/s, but the data are generally less reliable when wind speeds exceed 25 m/s (OSI SAF, 2019).

3 Quantifying interagency differences in the intensity of Lekima throughout its development

The intensity estimations by the JMA, CMA, and JTWC displayed different characteristics as Lekima developed. We therefore divided its life cycle into four intensity phases to discuss the differences between the three data sets (Fig. 2). Phase 1 was the formation stage (06:00 UTC on 2 August – 12:00 UTC on 4 August), when it developed from a tropical disturbance (TD) to a tropical storm (TS) with a MSW of 17.2 m/s. Lekima began as a TD located approximately 1000 km east of the Philippine in the

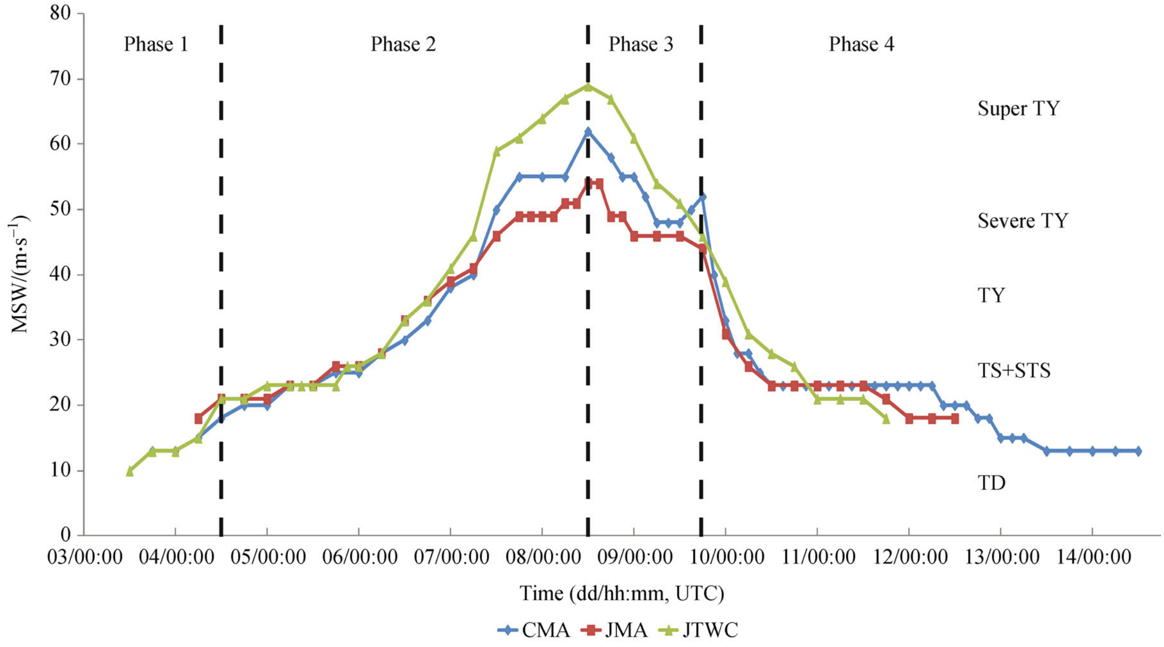

Fig. 2 Intensity estimations of Lekima in the three data sets (CMA, JMA, and JTWC). The intensity scales are classified by the CMA.

western North Pacific before moving north-westward. Using the JMA data set, Lekima intensified to a TS at 06:00 UTC on 4 August in the JMA data set, 6 h earlier than that in the CMA and JTWC data sets.

Phase 2 was the intensification phase (18:00 UTC on 4 August to 12:00 UTC on 8 August), defined as the period when Lekima went from being of TS intensity to reaching its peak MSW. In this phase, Lekima traced the south-western edge of a subtropical high, moving steadily to the north-west. The environmental conditions were favorable for TC development, and Lekima reached TY intensity (MSW > 32.6 m/s) on the evening of 7 August. During the next 36 h, Lekima intensified rapidly due to the favorable environment, which included a warm sea surface temperature, low vertical wind shear, and near-radial outflow. Lekima reached its peak intensity at 12:00 UTC on 8 August, located approximately 300 km east of Taiwan, China. Satellite images show that it maintained an annular structure, with a tightly compact convection ring surrounding a symmetric eye. The peak intensity in the JTWC data set was 69 m/s, which was larger than that in the CMA (62 m/s) and JMA (54 m/s) data sets.

Phase 3 (18:00 UTC on 8 August to 18:00 UTC on 9 August) was defined as the period from the time of peak intensity to the time Lekima made landfall in the Zhejiang Province. After reaching peak intensity, the surrounding convection became asymmetric with some erosion on the northern side and Lekima began to weaken. An eyewall replacement cycle likely began at 03:00 UTC on 9 August. However, the inner eyewall did not disappear, but strengthened prior to its landfall. Lekima made its landfall in the Zhejiang Province at 17:45 UTC on 9 August, having reached super typhoon intensity (52 m/s, 930 hPa) according to the CMA data set. The intensities just after landfall (18:00 UTC on 9 August) were 46 m/s and 44 m/s in the JTWC and JMA data sets, respectively.

Phase 4 was defined as the decay phase after Lekima's first landfall. According to the CMA and JMA data sets, Lekima weakened rapidly following landfall in the Zhejiang Province, and reached TS intensity ($17.2 \leqslant MSW < 24.5$ m/s) on the evening of 10 August. In contrast, the JTWC data set indicates that Lekima initially weakened relatively slowly after landfall, and then began to weaken much faster. According to the JTWC data set, Lekima dissipated in China's mainland on the morning of August 12. However, the CMA and JMA data sets indicate that Lekima maintained TS intensity until that date. During this period, the CMA best track data set shows that Lekima made landfall in the Shandong Province at 12:50 UTC on 11 August and again at 03:00 UTC on 12 August. Lekima then moved to and dissipated in the Bohai Bay, according to the CMA and JMA data sets.

To further explore the intensity discrepancies among these three data sets, the MSW differences are shown in Fig. 3 throughout Lekima's duration. The MSW values vary between data sets. For example, when the MSW_{CMA} was 23 m/s, the MSW_{JTWC} varied in the range 18–28 m/s (the subscript indicates the data set). Interagency differences are present for various TC intensities, but their magnitude is not always the same. The mean absolute errors (MAEs) were within 5 m/s when Lekima was weaker than severe TY intensity (MSW < 41.5 m/s), whereas for the high-intensity categories, noticeable differences were apparent, with $MSW_{JTWC} > MSW_{CMA} > MSW_{JMA}$. When Lekima

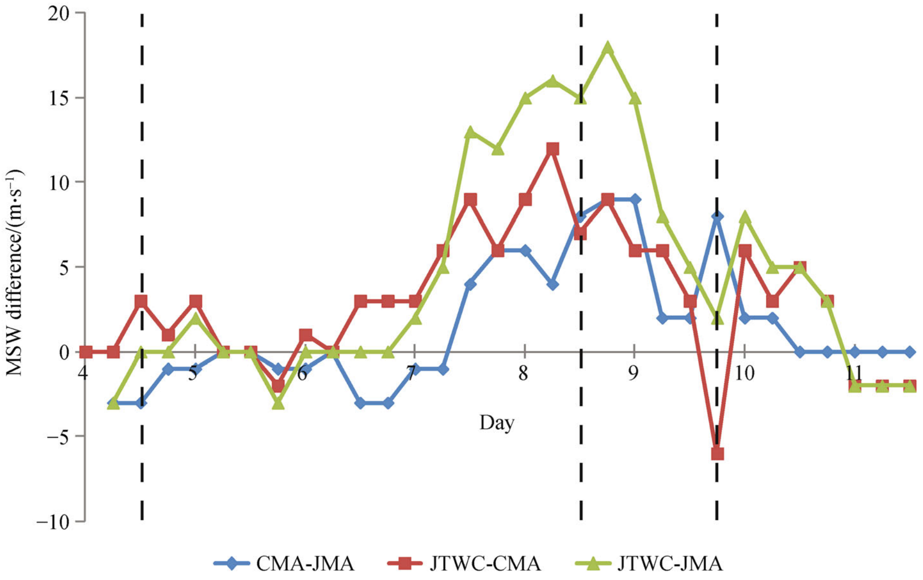

Fig. 3 TC intensity differences between the CMA, JMA and JTWC data sets.

reached its peak intensity, the MSW_{JTWC} was 69 m/s, which was 7 m/s and 15 m/s greater than the peak intensity in the CMA and JMA data sets, respectively. When Lekima made landfall in the Zhejiang Province, the MSW_{CMA} was 52 m/s, which was 6 m/s and 8 m/s stronger than the MSW_{JTWC} and MSW_{JMA}. As a result, Lekima at landfall was categorized as a super typhoon in the CMA data set, but as a severe typhoon in the JTWC and JMA data sets. After Lekima made landfall, the CMA and JMA data sets were almost consistent with one another regarding its intensity, whereas the MSW_{JTWC} was stronger within the first 24 h after Lekima made landfall, and then weakened much faster than in the other data sets.

One important difference among these data sets is that different averaging time intervals are used to calculate the MSW. Herein, we apply two methods to adjust the MSW definitions from 2-min (CMA) and 10-min (JMA) averages to a 1-min (JTWC) average. The first is the linear factor multiplication method, which considers the relationship between the 10-min and 1-min sustained wind speed to be linear, with a conversion factor of 1.14 (Atkinson, 1974). The MSW values from the CMA and JMA data sets multiplied by 1.14 are hereafter abbreviated as CMA×1.14 and JMA×1.14, respectively. The results are shown in Fig. 4(a). When the TC intensity was weaker than 52 m/s, the CMA×1.14 and JMA×1.14 MSWs were generally consistent with each other, but stronger than that of the MSW_{JTWC}. After Lekima reached super TY intensity (MSW > 52 m/s), the intensity differences became larger. CMA×1.14 and MSW_{JTWC} were generally consistent, and stronger than that of JMA×1.14. The second method we used is from Knapp and Kruk (2010). First, the MSW values were reversed back to a CI number based on the conversion coefficients used in each operational center. For example, the MSW_{CMA} (MSW_{JMA}) was reverted to CI numbers based on the CI–MSW conversions used in the CMA (JMA). Secondly, the Dvorak (1984) CI–MSW conversion table, which was used by the JTWC, was applied to convert from CI numbers to wind speeds (hereafter referred to as CMADT and JMADT). The results (Fig. 4(b)) will be discussed in detail in Section 3.1.

3.1 Phase 1: formation phase

The differences between the three data sets regarding the intensity of Lekima are most salient at two points during the formation phase (Fig. 1, Table 2). The first major difference is found during the period when the three agencies considered the circulation to be a TD. MSW values strengthened to a TD were estimated at 06:00 UTC on 2 August by the JMA, which was 30 h and 36 h earlier than that estimated by the JTWC and CMA, respectively. Another major difference is found during the period when the TD strengthened to a TS with a MSW greater than 17.2 m/s, which occurred at 06:00 UTC on 4 August in the JMA data set, 6 h earlier than that in the CMA and JTWC data sets.

Although each agency adopted the Dvorak approach to estimate Lekima's intensity, the MSW values were different. The details of the analysis procedure used to estimate the CI number from the same satellite data differed slightly among the three agencies. At the same time, there are some subjective differences between the analyses. The CI numbers from satellite data analysis provided by the satellite departments of the CMA and JMA (abbreviated as CCAA and RJTD) during the formation phase are shown in Table 2, alongside the time series of CI numbers obtained by the ADT. The CI numbers are about

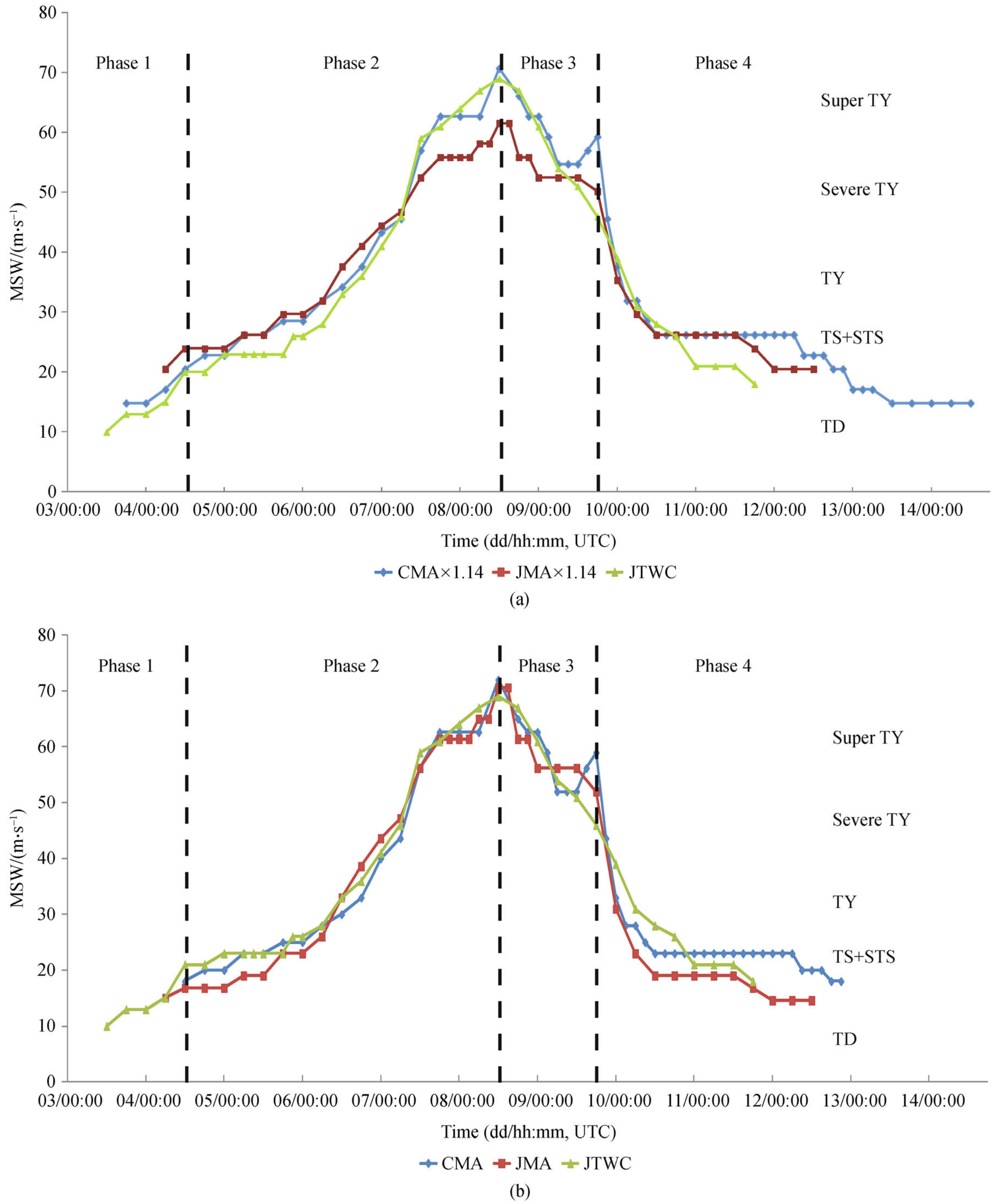

Fig. 4 Intensity of Lekima in the modified data sets: (a) CMA×1.14 (CMA original MSW multiplied by 1.14), JMA×1.14 (JMA original MSW multiplied by 1.14), and original JTWC MSW, (b) CMADT (CMA MSW using the Dvorak conversion table), JMADT (JMA MSW using the Dvorak conversion table), and original JTWC MSW.

2.0 at 06:00 UTC on 4 August according to the RJTD and ADT and are 2.5 at 12:00 UTC on 4 August according to both the CCAA and RJTD. As discussed earlier, the CI–MSW conversions were also independently established in each operational center (Fig. 1). A TC was classed as being of TS intensity when the CI number reached 2.0 in the JMA CI–MSW conversion table, while the CI number needed to be 2.5 in the JTWC and CMA CI–MSW conversion tables. Therefore, the time when the TD strengthened to a TS was earlier in the JMA data set. In addition, the MSW_{JMA} was generally stronger than the MSW_{CMA} and MSW_{JTWC} during the formation phase.

Table 2 The MSW and CI numbers during the formation phase in the different data sets

Variable	Agency	Time (UTC)		
		0406	0412	0418
MSW (m/s)	CMA	15	18	23
	JMA	18	21	21
	JTWC	15	21	21
CI number	CCAA	-	2.5	3.0
	RJTD	2.0	2.5	2.5
	ADT	1.9	2.4	2.3

Lekima initially formed from monsoon troughs, where it was embedded in a broad circulation and lacked deep convection near its center. Some studies (Velden et al., 2006) have noted that analysts need to avoid estimating the intensity of these kinds of TCs using the Dvorak technique, as the MSWs are too low if they are derived from the corresponding CI numbers. In the case of Lekima, the CI numbers from the objective analysis (i.e., the ADT) were actually smaller than those of the subjective analysis (CCAA and RJTD), which may be because the analysts took the underestimation of the Dvorak technique for this kind of TC into consideration. The ASCAT surface wind data showed a circulation with a large area of approximately 18–23 m/s westerly winds on the south side. When using the ASCAT surface wind speed as a baseline, the MSWs in these three best track data sets were of higher quality than those estimated by the ADT during this formation phase.

The results from adjusting the MSWs from 2-min (CMA) and 10-min (JMA) averages to a 1-min (JTWC) average are shown in Table 3. Both of the methods considered here enlarge the discrepancies between the JMA and JTWC MSW data sets. The application of the multiplicative factor enlarges the MSW difference between the CMA and JTWC data sets. The MSWs remain the same when applying the Dvorak CI–MSW conversion table to the CMA data set during the formation phase, since the CI–MSW conversion values are almost the same when the CI is less than 4.0 in the CMA table and Dvorak table. These results indicate that in addition to the different CI numbers, the difference in the CI–MSW conversion table was the other main source of discrepancy in TC intensity between the JMA and JTWC data sets during the formation phase. The TC intensity difference between the CMA and the JTWC data sets was mainly related to the CI discrepancies.

3.2 Phase 2: intensification phase

The interagency differences were large during the intensification phase (Fig. 3). When the TC intensity was between 24.5 and 41.4 m/s, the MSWs in the three data sets were generally consistent with one another. When Lekima reached severe TY intensity (MSW ⩾ 41.5 m/s), the MSW_{JTWC} was generally stronger than the MSW_{CMA} and MSW_{JMA}. Moreover, stronger intensities tended to lead to larger differences between the data sets. The largest differences between the MSW_{JTWC} data set and the MSW_{JMA} and MSW_{CMA} data sets were 18 m/s and 12 m/s, respectively (Fig. 3). Our results suggest that the intensity of strong (weak) TCs in the JTWC data set is generally greater (smaller) than that in the CMA and JMA data sets. This distribution characteristic is consistent with the results of previous studies, which analyzed large samples of historical TCs (Song et al., 2010; Wu et al., 2006).

Table 3 The mean absolute error (MAE) and the largest absolute error (LAE) between the JTWC, CMA, and JMA data sets during different phases. The errors are calculated based on the common records included in the two compared data sets

		JTWC vs CMA		JTWC vs JMA	
		MAE	LAE	MAE	LAE
Phase 1	Original MSW (m/s)	1.0	3.0	1.5	3.0
	MSW1m (m/s)	1.3	2.0	4.5	6.0
	MSWDT (m/s)	1.0	3.0	2.0	4.0
	CI number	0.2	0.3	0.3	0.5
Phase 2	Original MSW (m/s)	4.1	12.0	5.2	16.0
	MSW1m (m/s)	2.3	6.0	4.7	9.0
	MSWDT (m/s)	1.8	4.0	2.5	6.0
	CI number	0.2	0.3	0.2	0.7
Phase 3	Original MSW (m/s)	3.0	9.0	9.6	18.0
	MSW1m (m/s)	4.2	13.0	5.4	11.0
	MSWDT (m/s)	4.0	13.0	4.8	6.0
	CI number	0.3	1.0	0.4	0.6

Adjusting the MSWs from 2-min (CMA) and 10-min (JMA) averages to a 1-min (JTWC) average by remapping with the Dvorak CI–MSW conversion table decreased the interagency intensity discrepancies between the three best track data sets. On the other hand, multiplying the MSW_{CMA} and MSW_{JMA} by 1.14 increased the interagency intensity discrepancies with the JTWC data set for MSWs less than 30 m/s, but decreased the discrepancies slightly for larger MSWs during the intensification phase (Fig. 4). The largest absolute error (LAE) decreased from 12 m/s and 16 m/s to 6 m/s and 9 m/s between the JTWC data set and the CMA and JMA data sets, respectively. Recalculating the MSW_{JMA} from the CI numbers with the Dvorak CI–MSW conversion table reduced the interagency discrepancies significantly between the JMA and JTWC data sets, with the MAE and LAE decreasing from 5.2 m/s and 16 m/s to 2.5 m/s and 6 m/s, respectively. This method also decreased the MAE and LAE for CMA–JTWC from

4.1 m/s and 12 m/s to 1.8 m/s and 4 m/s, respectively. The peak intensity of Lekima was 62 m/s, 54 m/s, and 69 m/s in the original CMA, JMA, and JTWC data sets, respectively. After adjusting the MSW definition to a 1-min average, the peak intensity of Lekima in the CMA data set was 71 m/s when using the linear factor method and 72 m/s when using the Dvorak CI–MSW conversion table method. The JMADT was systematically stronger than JMA×1.14 for high MSWs, with peak intensities of 71 m/s and 62 m/s, respectively. The Dvorak CI–MSW conversion table method significantly decreases interagency discrepancies in the intensity of Lekima, indicating that the use of different CI–MSW conversion tables was the main cause of those discrepancies during the intensification phase.

3.3 Phase 3: 24 h before landfall

After Lekima reached its peak intensity at 12:00 UTC on 8 August, it continued north-westward to Eastern China. The satellite images showed a small distinct pinhole eye surrounded by a narrow intense convective ring during the rapid intensification and peak intensity period. However, the surrounding convection became asymmetric with warmer cloud-top temperatures on the northern side, indicating that Lekima began to weaken. The weakening trend was consistent in the three data sets, but there were still noticeable differences in the MSW, with $MSW_{JTWC} > MSW_{CMA} > MSW_{JMA}$. During the next 12 h, there was an obvious discrepancy in the intensity trend among the three data sets. Whereas the intensity continued to weaken at the same rate in the JTWC data set, in the JMA data set, the intensity was maintained at 46 m/s for several hours, and then slightly weakened to 44 m/s. In contrast, Lekima strengthened just before landfall in the CMA data set, with a MSW of 48 m/s increasing to 52 m/s.

The remapping method based on the Dvorak conversion table was particularly effective at reducing the differences between the JMA and JTWC data sets, with the MAE (LAE) decreasing from 9.6 m/s (18 m/s) to 4.8 m/s (6 m/s) in this phase. Table 3 also shows that the MAE and LAE between the JTWC and JMADT data sets were larger in the decaying phase (phase 3) than in the intensification phase (phase 2). These results indicate that apart from different tables for CI–MSW conversion, CI discrepancies also contributed to intensity differences between the JTWC and JMA data sets during phase 3, which can be related to the different analysis procedures used for decaying TCs by each agency. However, both methods to unify the wind averaging period failed to reduce discrepancies between the CMA and JTWC data sets during this phase, which indicates that there are some other important contributing factors related to the use of different observational data sources by these two agencies.

The CI numbers issued by the different agencies were compared from 12:00 UTC to 18:00 UTC on 9 August. During this time, the CI numbers issued by the JMA satellite message increased from 5.0 to 5.5. This intensification trend was also found in the CI numbers obtained using the DDIE method, with the numbers increasing from 4.3 to 4.9. However, the CI numbers obtained through the ADT slightly weakened from 5.0 to 4.8. The reason for these CI discrepancies could be related to Lekima's structure, since the concentric eyes and eyewall replacement cycle, which were linked to its intensity, were not included in the original Dvorak model (Velden et al., 2006).

Satellite images showed that Lekima likely began an eyewall replacement cycle at 03:00 UTC on 9 August, when a new eyewall formed outside the original small eyewall. This new outer eyewall then contracted and the inner eyewall began to weaken. However, the inner eyewall did not disappear, but strengthened after 09:00 UTC on 9 August (Fig. 5). The inner eye was still a prominent feature, suggesting that the eyewall replacement cycle was not complete. Lekima was strengthened just before landfall in Eastern China, with a more well-defined eyewall. This intensification trend was shown in the CMA data set.

When Lekima made landfall in the Zhejiang Province, the 2-min MSW_{CMA} was 52 m/s at 17:45 UTC on 10 August, which is 6 m/s and 8 m/s greater than the 1-min MSW_{JTWC} and 10-min MSW_{JMA}, respectively, at 18:00 UTC on 10 August. The MSW values were reversed back to the CI based on the conversion tables used in the respective operational center. The CI number calculated from the 10-min MSW_{JMA} was 5.5, which was consistent with the CI number provided by the JMA satellite message. The CI number of the 1-min MSW_{JTWC} was 5.0, which was nearly the same as that suggested by the ADT (4.8) and DDIE (4.9). The CI number of the 2-min MSW_{CMA} was 6.0, which was larger than that of the other two data sets. As mentioned earlier, the concentric eyes and eyewall replacement process were not included by the original Dvorak model. Velden et al. (2006) noted that Hurricane Charley (2004) was underestimated by the Dvorak technique owing to an eyewall replacement cycle and contraction of the eye. Therefore, the forecasters relied mainly on aircraft observational data for landfalling TCs in the Atlantic, rather than satellite images (Velden et al., 2006). Although there were no aircraft data for Lekima, there were a large number of automatic surface weather stations over the land area of China.

Figure 6 shows the sea surface pressure observed by two automatic surface weather stations, which were located at Aohuan of Zhejiang and Sansuan Island of Zhejiang. At 17:00 UTC on 9 August, the TC center was located on the western side of Sansuan Island at a distance of approximately 14 km, and on the south-eastern side of the Aohuan observatory at a distance of 13 km. The sea surface pressures observed by these two stations were almost the same (941.4 hPa and 941.6 hPa) at this time. These results indicate that the pressure gradient was constant on the

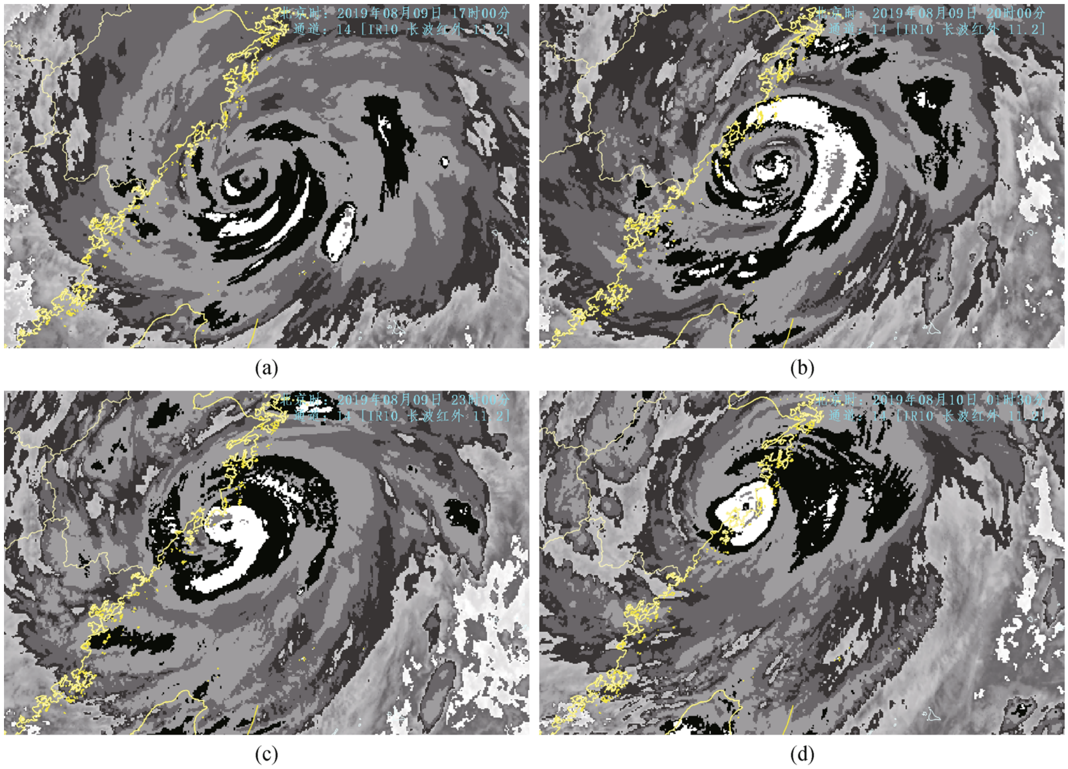

Fig. 5 Satellite images for Lekima at (a) 09:00 UTC on 9 August, (b) 12:00 UTC on 9 August, (c) 15:00 UTC on 9 August, and (d) 17:30 UTC on 10 August observed by Himawari-8. The grayscale indicates the brightness temperature of infrared satellite images.

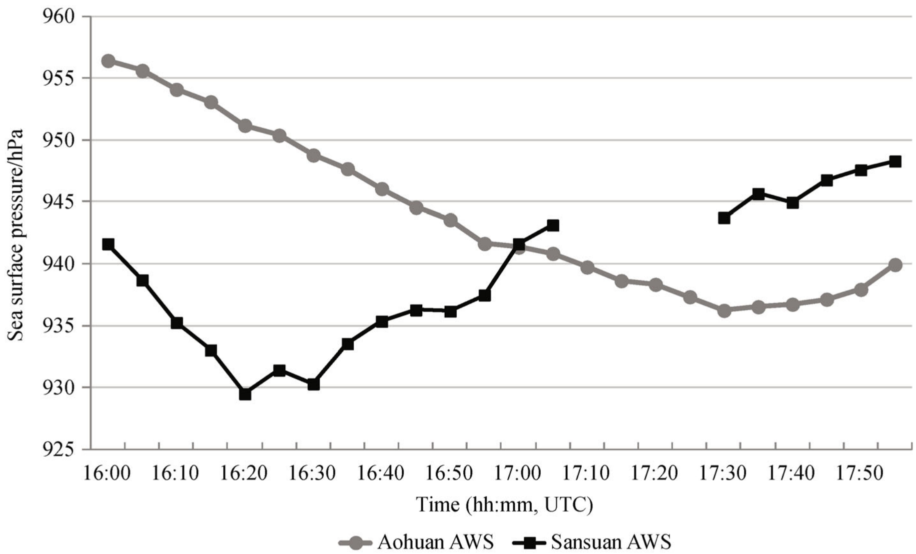

Fig. 6 The sea surface pressure observed on 9 August by two automatic surface weather observation stations, which were located in Aohuan of Zhejiang and on Sansuan Island of Zhejiang.

northern and eastern sides of the TC center, which means that inner-core structures of Lekima were still relatively symmetric at this time. The lowest sea surface pressure observed on Sansuan Island was approximately 930 hPa at 16:20 UTC, located approximately 12 km from the TC center, which indicates that the minimum sea surface pressure of Lekima was not higher than 930 hPa at this time. The lowest sea surface pressure observed at the Aohuan observatory was 936 hPa, located approximately 2 km from the TC center at 18:00 UTC. Therefore, the MSLP of 930 hPa at landfall in the CMA data set was reasonable, while the MSLP of 950 hPa in the JMA data set was too high.

Based on the WPRs used by the CMA (Ying, et al., 2014), the JMA (Koba et al., 1991), and Dvorak technique (1975), the MSWs were converted to 60 m/s (2-min), 50 m/s (10-min), and 65 m/s (1-min), respectively, when the MSLP was 930 hPa. Kossin (2015) suggested that the MSW may be overestimated for TCs that experienced an eyewall replacement cycle when using surface pressure measurements on land and existing WPRs. This would imply that the actual intensity of Lekima was slightly weaker than the MSW calculated by the existing WPRs. The 2-min averaged maximum wind speed was observed as 50.5 m/s on Sansuan Island (station height 79 m) at 17:50 UTC, with a peak gust of 61.4 m/s. Earlier studies (Nolan et al. 2014) found that the actual peak intensity is underestimated by 5%–20% when anemometers experience a direct hit by the right side of the eyewall. This would suggest that the actual intensity of Lekima was stronger than the observed wind speed.

Lekima's intensity was discussed by the working group of Experts on Typhoon and Marine Meteorology at the work conference of the CMA, which was a very important step in determining the CMA best track data. The work conference mainly dealt with the analysis difficulties related to TC tracks, intensities, and landfall information. Taking into account the surface observation data, the Dvorak intensity estimation, and the intensity trend, the MSW of Lekima at landfall was set as 52 m/s, with a MSLP of 930 hPa in the CMA best track data.

3.4 Phase 4: After landfall

After landfall in the Zhejiang Province, Lekima moved northward and weakened rapidly to TS intensity (17.2⩽MSW < 24.5 m/s) in the CMA and JMA data sets. The MSW_{JTWC} initially weakened more slowly after landfall, and then weakened faster (Fig. 2). During this phase, the MSW and MSLP in the CMA data set were almost identical with those in the JMA data set, with a MAE of 1.6 m/s and 0.9 hPa, respectively (Fig. 7). However, there were larger differences between the MSW_{JTWC} and the MSW_{CMA} and MSW_{JMA}, with MAEs of 3.8 m/s and 3.6 m/s, respectively.

To evaluate which data set provides more accurate estimations, the surface observations are also shown in Fig. 7. The pressure shown in Fig. 7 is the lowest pressure observed by the automatic surface weather station at heights less than 50 m and within 50 km of the TC center. Also shown is the strongest wind observed by the automatic surface weather station at heights less than 50 m and within 200 km of the TC center. The MSLP in the CMA data set was almost identical to the observations, with a mean absolute error of 1.7 hPa. The MSW in the CMA data set was also close to the observations, but always higher than in the observational data. The MSW and MSLP in the JMA data set were very consistent with the observational data. However, the MAE between MSW_{JTWC} and the observed wind speed was relatively large at 6.0 m/s.

4 Summary and conclusions

In this paper, we quantified differences in intensity estimations of Typhoon Lekima (2019) throughout its development between the data sets of three different agencies: the CMA, JMA, and JTWC. The results show that there were significant discrepancies in the intensity estimations of Lekima between the three operational centers. The maximum differences were 16 m/s and 12 m/s between the JTWC data set and the JMA and CMA data sets, respectively, at 06:00 UTC on 8 August,

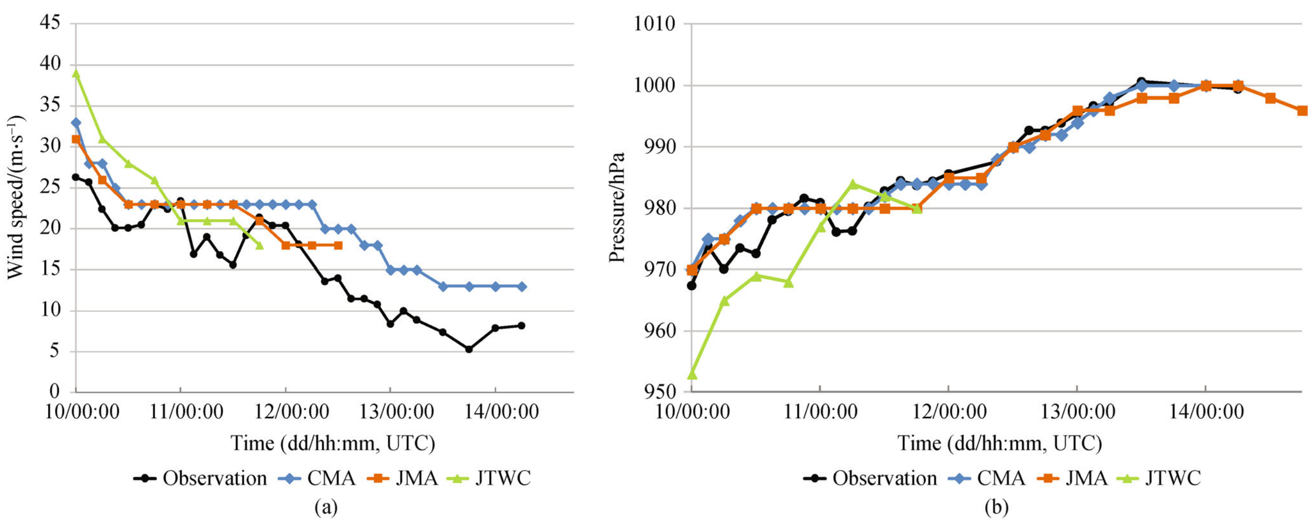

Fig. 7 (a) The observed wind speed and the MSW in the CMA, JMA, and JTWC data sets, (b) the observed pressure and the MLSP of the data sets after Lekima made landfall.

just before Lekima reached its peak intensity. The magnitude of the interagency differences varied with the intensity of Lekima. When Lekima reached severe TY intensity in the ocean, the MSW_{JTWC} was generally stronger than the MSW_{CMA} and MSW_{JMA}, that is $MSW_{JTWC} > MSW_{CMA} > MSW_{JMA}$.

The ability of two distinct methods to minimize the differences between these three data sets was also evaluated. Both the remapping method based on the original Dvorak CI–MSW conversion table and the linear factor multiplication method (CMA×1.14, JMA×1.14) substantially reduced intensity discrepancies, with the former method being particularly effective, though only during the intensification phase over the ocean. In the decaying phase, remapping the MSWs based on the original Dvorak conversions did reduce the intensity discrepancies between the JMA and the JTWC wind speeds somewhat, but a relatively large difference nevertheless remained. The results indicate that apart from different CI number–MSW conversions, CI discrepancies also contributed to differences between the MSW_{JTWC} and the MSW_{JMA} during the TC decay phase.

Lekima made landfall in the Zhejiang Province of China at 17:45 UTC on 10 August, with a MSW_{CMA} of 52 m/s, which was 6 m/s and 8 m/s greater than the MSW_{JTWC} and MSW_{JMA}, respectively, at 18:00 UTC on 9 August. Both methods intended to unify the wind averaging period did not reduce discrepancies between the intensity recorded just before landfall by the CMA and the other two agencies. This indicates that there were some other important contributing factors related to the use of different observational data sources by each agency. The landfall intensity of Lekima in CMA best track data set was determined by taking into account of the surface observation data (wind speed and pressure), the Dvorak intensity estimation, and the intensity trend.

To evaluate the intensity estimations of these three data sets, we compared them to surface station observations and ASCAT sea-surface winds. During the formation phase, the TD strengthened to a TS earlier in the JMA data set than in the other two data sets. When Lekima made its landfall in China, the CMA data set had more complete information, including the landfall location, date, time, and landfall intensity. In addition, the CMA data set included a large amount of surface weather observation data over land in China, making it advantageous for TCs that make landfall. When Lekima passed over land in China, the MSW and MSLP in the CMA data set were recorded according to the surface observations, and were very consistent with the JMA data set. However, there were remarkable MSW differences between the JTWC data set and the CMA and JMA data sets during this phase.

It is important to document different operational procedures and input data that are used for TC intensity estimations by various operational agencies, otherwise studies and forecasts based on best track data may be misleading. Although the Dvorak technique is still the standard method for TC intensity estimations when other direct observational data are not available, this technique has several limitations. As mentioned in this paper, it may underestimate the TC intensity when TCs form in a monsoon trough or when TCs undergo an eyewall replacement cycle. Therefore, direct observations of offshore TCs need to be performed, as this would help to provide a more accurate TC intensity data set and reduce intensity discrepancies between different agencies.

Acknowledgements We thank the meteorological observers, forecasters, and experts from within and outside of CMA, who were and are devoted to the construction of the database, for their hard work on data collection, processing, and analysis. This research was supported jointly by the Key Program for International S&T Cooperation Projects of China (No. 2017YFE0107700), and the National Natural Science Foundation of China (Grant Nos. 41875080 and 42075056).

References

Atkinson G D (1974). Investigation of gust factors in tropical cyclones. FLEWEACENTech. Note JTWC 74–1, Fleet Weather Center, Guam

Atkinson G D, Holliday C R (1977). Tropical cyclone minimum sea level pressure/maximum sustained wind relationship for the western North Pacific. Mon Wea Rev, 105: 421–527

Bai L, Yu H, Black P G, Xu Y, Ying M, Tang J, Guo R (2019). Reexamination of the tropical cyclone wind–pressure relationship based on pre-1987 aircraft data in the western North Pacific. Weather Forecast, 34(6): 1939–1954

Barcikowska M, Feser F, von Storch H (2012). Usability of best track data in climate statistics in the western North Pacific. Mon Weather Rev, 140(9): 2818–2830

China Meterological Administration (2012). Typhoon Operational Performance and Service Regulations. Beijing: China Meteorological Press (in Chinese)

Dvorak V F (1975). Tropical cyclone intensity analysis and forecasting from satellite imagery. Mon Weather Rev, 103(5): 420–430

Dvorak V F (1984). Tropical cyclone intensity analysis using satellite data. NOAA/NESDIS Tech. Rep. 11

Group of Satellite Imagery Analysis (1980a). Methods for typhoon prediction using the satellite imagery (I). Meteorol Mon, 6: 24–26 (in Chinese)

Group of Satellite Imagery Analysis (1980b). Methods for typhoon prediction using the satellite imagery (II). Meteorol Mon, 6: 25–27 (in Chinese)

Kang N Y, Elsner J B (2012). Consensus on climate trends in western north pacific tropical cyclones. J Clim, 25(21): 7564–7573

Knaff J A, Zehr R M (2007). Reexamination of tropical cyclone wind–pressure relationships. Weather Forecast, 22(1): 71–88

Knapp K R, Kruk M C (2010). Quantifying interagency differences in tropical cyclone best-track wind speed estimations. Mon Weather Rev, 138(4): 1459–1473

Koba H, Hagiwara T, Osano S, Akashi S (1991). Relationships between CI number and minimum sea level pressure/maximum wind speed of tropical cyclones. Geophys Mag, 44: 15–25

Kossin J P (2015). Hurricane wind–pressure relationship and eyewall replacement cycles. Weather Forecast, 30(1): 177–181

Liu Y M (2015). Application of inner verification sequence alignment model to two data source splicing of AWS hourly precipitation. Meteorol Mon, 41: 1398–1407

Lu X Q, Yu H (2013). An objective tropical cyclone intensity estimation model based on digital IR satellite images. Trop Cyclone Res Rev, 2: 233–241

Lu X Q, Yu H, Yang X M, Li X F, Tang J (2019). A new technique for automatically locating the center of tropical cyclones with multi-band cloud imagery. Front Earth Sci, 13(4): 836–847

Nolan D S, Zhang J A, Uhlhorn E W (2014). On the limits of estimating the maximum wind speeds in hurricanes. Mon Weather Rev, 142(8): 2814–2837

Olander T L, Velden C S, Kossin J P (2004). The advanced objective dvorak technique (AODT)-continuing the journey. In: 26th AMS Conf. on Hurricane and Tropical Meteorology, Miami, FL, USA

Olander T L, Velden C S (2007). The advanced Dvorak technique: Continued development of an objective scheme to estimate tropical cyclone intensity using geostationary infrared satellite imagery. Weather Forecast, 22(2): 287–298

OSI SAF (2019). ASCAT Wind Product User Manual

Ren F, Liang J, Wu G, Dong W, Yang X (2011). Reliability analysis of climate change of tropical cyclone activity over the western North Pacific. J Clim, 24(22): 5887–5898

Sivareddy S, Ravichandran M, Girishkumar M S (2013). Evaluation of ASCAT-Based daily gridded winds in the tropical Indian Ocean. J Atmos Ocean Technol, 30(7): 1371–1381

Song J J, Wang Y, Wu L (2010). Trend discrepancies among three best track datasets of western North Pacific tropical cyclones. J Geophys Res, 115(D12): D12128

U.S. Fleet Weather Facility (2007). Annual Tropical Storm Report. U.S. Fleet Weather Facility, Miami, FL

Velden C, Harper B, Wells F, Beven J L II, Zehr R, Olander T, Mayfield M, Guard C C H I P, Lander M, Edson R, Avila L, Burton A, Turk M, Kikuchi A, Christian A, Caroff P, McCrone P (2006). The Dvorak tropical cyclone intensity estimation technique: a satellite-based method that has endured for over 30 years. Bull Am Meteorol Soc, 87 (9): 1195–1210

Wu M C, Yeung K H, Chang W L (2006). Trends in western North Pacific tropical cyclone intensity. Eos (Wash DC), 87(48): 537–538

Xu Y L, Zhang L, Xiang C Y (2015). Typhoon intensity estimation technique and its operational application: with example of Dvorak technique. Adv Met S & T, 5: 22–34 (in Chinese)

Yeung K H (2006). Issues related to global warming—myths, realities and warnings. In: the 5th Conference on Catastrophe in Asia, Hong Kong Obs, Hong Kong, China

Ying M, Cha E, Kwon H (2011). Comparison of three western North Pacific tropical cyclone best track datasets in a seasonal context. J Meteor Soc Japan, 89(3): 211–224

Ying M, Zhang W, Yu H, Lu X, Feng J, Fan Y, Zhu Y, Chen D (2014). An overview of the China Meteorological Administration tropical cyclone database. J Atmos Ocean Technol, 31(2): 287–301

Yu H, Hu C, Jiang L (2007). Comparison of three tropical cyclone strength datasets. Acta Meteorol Sin, 64: 357–363

Yu H, Chen L S (2019). Impact assessment of landfalling tropical cyclones: introduction to the special issue. Front Earth Sci, 13(4): 669–671

Zehr R (1989). Improved objective satellite estimates of tropical cyclone intensity. In: 18th Conf on Hurricanes and Tropical Meteorology, San Diego, CA. Amer Meteor Soc, J25–J28